

Nucleation and growth of platelets in hydrogen-ion-implanted silicon

Michael Nastasi, Tobias Höchbauer, Jung-Kun Lee, Amit Misra, John P. Hirth, Mark Ridgway, and Tamzin Lafford

Citation: [Applied Physics Letters](#) **86**, 154102 (2005); doi: 10.1063/1.1900309

View online: <http://dx.doi.org/10.1063/1.1900309>

View Table of Contents: <http://scitation.aip.org/content/aip/journal/apl/86/15?ver=pdfcov>

Published by the [AIP Publishing](#)

Articles you may be interested in

[Selective nucleation induced by defect nanostructures: A way to control cobalt disilicide precipitation during ion implantation](#)

J. Appl. Phys. **112**, 123504 (2012); 10.1063/1.4769213

[Role of strain in the blistering of hydrogen-implanted silicon](#)

Appl. Phys. Lett. **89**, 101901 (2006); 10.1063/1.2345245

[Hydrogen gettering and strain-induced platelet nucleation in tensilely strained Si_{0.4}Ge_{0.6}/Ge for layer exfoliation applications](#)

J. Appl. Phys. **97**, 104511 (2005); 10.1063/1.1900928

[Thermal activation of As implanted in bulk Si and separation by implanted oxygen](#)

J. Appl. Phys. **96**, 7388 (2004); 10.1063/1.1776319

[Improved depth profiling with slow positrons of ion implantation-induced damage in silicon](#)

J. Appl. Phys. **94**, 4382 (2003); 10.1063/1.1606855

An advertisement for Asylum Research Cypher AFMs. The background is a dark blue gradient with a film strip on the left side. The text is in white and orange. The main text reads: 'Not all AFMs are created equal', 'Asylum Research Cypher™ AFMs', and 'There's no other AFM like Cypher'. At the bottom, there is a website URL and the Oxford Instruments logo with the tagline 'The Business of Science®'.

Not all AFMs are created equal

Asylum Research Cypher™ AFMs

There's no other AFM like Cypher

www.AsylumResearch.com/NoOtherAFMLikeIt

OXFORD
INSTRUMENTS
The Business of Science®

Nucleation and growth of platelets in hydrogen-ion-implanted silicon

Michael Nastasi,^{a)} Tobias Höchbauer, Jung-Kun Lee, Amit Misra, and John P. Hirth
*Material Science and Technology Division, Los Alamos National Laboratory,
 Los Alamos, New Mexico 87545 USA*

Mark Ridgway
Australian National University, Canberra ACT 0200, Australia

Tamzin Lafford
Bede Scientific Instruments Ltd., Durham, DH1 1TW, United Kingdom

(Received 4 January 2005; accepted 7 March 2005; published online 5 April 2005)

H ion implantation into crystalline Si is known to result in the precipitation of planar defects in the form of platelets. Hydrogen-platelet formation is critical to the process that allows controlled cleavage of Si along the plane of the platelets and subsequent transfer and integration of thinly sliced Si with other substrates. Here we show that H-platelet formation is controlled by the depth of the radiation-induced damage and then develop a model that considers the influence of stress to correctly predict platelet orientation and the depth at which platelet nucleation density is a maximum. © 2005 American Institute of Physics. [DOI: 10.1063/1.1900309]

The introduction of hydrogen into single crystalline Si is known to result in the precipitation of planar defects in the form of platelets. When H is introduced into Si by diffusion through plasma hydrogenation these platelets form only on {111} crystallographic planes independent of the Si crystal orientation.¹ In sharp contrast to that case, when H⁺ ions are implanted into (100) Si, platelets are observed on (100) that are parallel to the surface and on {111} planes with the majority being of the (100) type.² These H platelets are typically a few tens of nanometers in size and are considered to be composed of a two-dimensional array of H–Si bonds. Understanding how these platelets form is important since they are necessary for the planar cleavage of silicon that allows liftoff and transfer of thin single crystalline sheets that can, in principle, be heterogeneously integrated with virtually any substrate. Here we show that in the case of H ion implantation into (100) and (111) Si, the predominant platelet orientation is parallel to the substrate surface, perpendicular to the *z* (normal) direction of the substrate. These observations are rationalized using stress and strain dependent models of nucleation and growth.

H ions were implanted into (100) and (111) *p*-type single crystal Si at an energy of 42 keV and dose of 3×10^{16} H/cm². The Si substrates were held at liquid nitrogen temperature during the implantation. To minimize effects of ion channelling during the implantation process, the incident ion beam was oriented at 7° from the surface normal. Following the ion implantation step the H implanted wafer underwent a thermal anneal at 380 °C for 30 mins in vacuum.

The sample was characterized in detail in the as-implanted state and also after annealing. Rutherford back-scattering spectroscopy in the channeling mode was used to analyze the radiation-induced damage accumulation. Channeling measurements were obtained with a 2.0 MeV ⁴He⁺ analyzing beam and a detector located 13° from the incident beam. Elastic recoil detection analysis was performed to measure the hydrogen depth distribution in the as-implanted

sample using a 3.0 MeV ⁴He⁺ analyzing beam. The analyzing beam was oriented 75.25° from the sample normal. The detector was positioned 150.5° from the incident beam. A laser beam was used to consistently align the samples with respect to the analyzing beam and the detector. The laser alignment provided an accuracy of $\pm 0.05^\circ$ for the angles between the analyzing beam, the sample surface, and the detector. To avoid detection of forward-scattered α particles, a 20 μ m thick Mylar foil was placed between the sample and the hydrogen detector.

Detailed microstructural information about the defects generated during H-ion implantation was obtained by cross-section transmission-electron microscopy (XTEM) in the as-implanted state and also after annealing. TEM analysis was carried out on a Philips CM 30 operated at 300 kV.

The strain depth distribution in the samples after the H implantation was measured by means of double crystal x-ray diffraction. Double crystal ω - 2θ scans were collected using a Bede QC200 fitted with a 1.5 mm high performance polycapillary optic and a Ge 004 reference crystal. The scans were auto-fitted using BEDE RADS software to obtain the depth-strain profiles.³

Figure 1 shows the ion implantation damage distribution in hydrogen as-implanted (100) silicon. This profile was reduced from ion channeling data using the method described by Nastasi *et al.*⁴ The data show that the damage is peaked at 408 nm with a variance of approximately 130 nm. Also plotted in Fig. 1 is the depth distribution of out-of-plane strain ϵ_{zz} , as measured by double crystal x-ray diffraction and the implanted hydrogen distribution, measured by elastic recoil detection.^{5,6} A comparison of the data presented in Fig. 1 shows that the strain is well correlated with the ion implantation damage, consistent with previous work,^{7,8} and that these distributions peak at a lower depth than the peak in the hydrogen distribution.

The cross-sectional transmission electron microscopy (TEM) images presented in Fig. 2 show that platelets do not form in silicon implanted with hydrogen at liquid nitrogen temperatures. However, plateletlike defects are observed in both (100) and (111) silicon after annealing. For the (100)

^{a)} Author to whom all correspondence should be addressed; electronic mail: nasty@lanl.gov

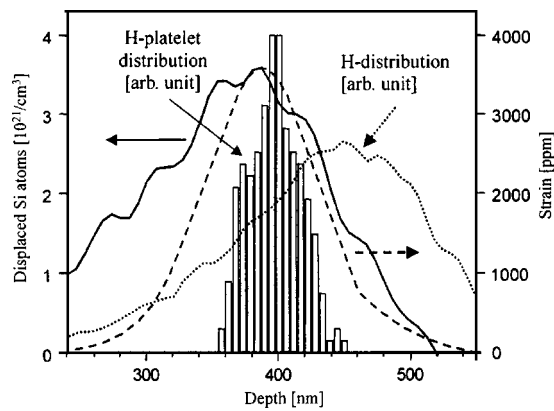


FIG. 1. Experimental data from hydrogen as-implanted (100) silicon. The solid curve is the ion implantation damage distribution, obtained from ion channelling data. The dashed curve is the out-of-plane strain distribution ϵ_{zz} , as measured by double crystal x-ray diffraction, and the dotted curve is the implanted hydrogen distribution, measured by elastic recoil detection. Also presented is a histogram showing the distribution of (100) platelets, which was obtained from an analysis of the TEM data shown in Fig. 2.

silicon a dense band of platelets with a (100) crystal orientation are observed at a depth of approximately 360 to 420 nm with few {111} oriented platelets apparent at a depth of 410 nm. For the (111) Si, only (111) platelets are observed in the depth interval between 360 and 450 nm. In both substrates, the predominant platelet orientation is parallel to the substrate surface and perpendicular to the out-of-plane strain.

A histogram showing the distribution of (100) platelets in (100) Si, as observed in Fig. 2, is presented in Fig. 1. The platelet distribution is coincident with the implantation damage and strain distributions. A similar trend is expected for the hydrogen implanted (111) silicon. The data presented in Fig. 1, together with the TEM data presented in Fig. 2, suggests that platelet orientation in hydrogen ion implanted silicon is strongly affected by ion implantation damage and the resulting strain distribution.

Earlier results presented by Höchbauer *et al.*² and Zheng *et al.*⁹ showed that the lattice damage produced by H ion implantation into Si results in the formation of an in-plane biaxial compressive (negative) stress. Höchbauer observed the correlation between the platelet and damage distribution^{10,11} and proposed that the out-of-plane tensile strain ϵ_{zz} that would accompany an in-plane compressive stress $\sigma_{xx} = \sigma_{yy}$, would be peaked at the location of maximum damage and that the strain assists in nucleating Si-H defects that evolve into H platelets.¹² Reboredo and coworkers¹³ have used first-principles calculations to examine the energetics of different hydrogen defect complexes in silicon and concluded that aggregates of VH_4 (four hydrogen atoms attached to a silicon vacancy) are the precursors to platelet formation and that the formation energy of VH_4 defects decreases in the presence of a tensile strain. However, the nucleation and kinetic pathway to forming these aggregates under ion implantation conditions was not explored. A key finding in this work¹³ is that the complex produces asymmetrical tensile displacement, equivalent to a point force dipole oriented in the z direction,¹⁴ in contrast to the vacancy alone, which is expected to produce isostatic compressive displacement. The surrounding matrix strain field is compressive in the z direction.

Given the nonequilibrium spatial variations in defects and strain found in our as-implanted samples, a flux of de-

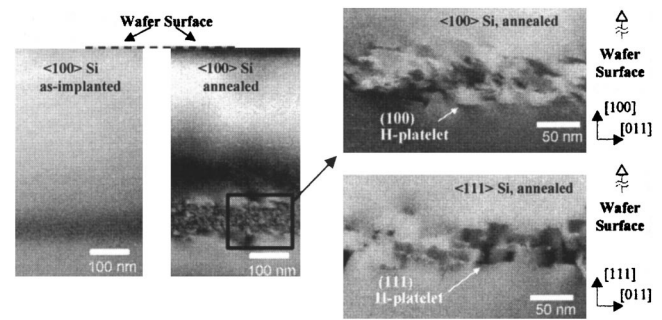


FIG. 2. Cross-sectional TEM micrographs from implanted and annealed Si. Platelets are not observed in silicon implanted with hydrogen at liquid nitrogen temperatures but are present in both (100) and (111) silicon after annealing. For both substrates, the predominant platelet orientation is parallel to the substrate surface and perpendicular to the out-of-plane strain direction and the projected range of the implanted hydrogen.

fects will occur upon annealing. Relief of the implantation induced out-of-plane strain will be efficiently accomplished by Si-Si bond breaking, which provides a driving force for a vacancy flux toward the peak in the strain distribution. This flux will be countered by the vacancy flux away from the peak in the damage distribution due to the damage concentration gradient. The total vacancy flux J in the out-of-plane (z) direction can be described by¹⁵

$$J = -D \left(\frac{dc}{dz} + \frac{c}{k_B T} \frac{dF}{dz} \right), \quad (1)$$

where D is the vacancy diffusion coefficient, c is the concentration of vacancies, and dc/dz is the vacancy concentration gradient, dF/dz is the potential field gradient that arises from the strain energy on atoms in the strained region of the lattice, and includes contributions from the complete strain tensor. A corresponding equation for the flux of interstitials will also exist. However, since the addition of interstitial atoms to a strained region increases the strain, both terms in the flux equation will move interstitials away from the damage and strain peaks. Therefore, the presence of an out-of-plane tensile strain ϵ_{zz} leads to a maximum supersaturation in vacancies prior to platelet nucleation at the peak in the strain distribution, where the hydrogen concentration is also large. As vacancies are consumed in the nucleation and growth of platelets the local concentration of free vacancies diminishes, creating a local vacancy sink. Under these conditions the dc/dz term in Eq. (1) is dominant in the diffusion of vacancies into the region of highest platelet density.

On the basis of the present experimental data and analysis, vacancies clearly are predisposed to migrate to the region of highest out-of-plane strain. Silicon vacancies are extremely mobile during the 380 °C anneal¹⁶ and calculations suggest that the VH_1 defect may be mobile in silicon but with a higher activation energy than the pure vacancy.¹⁷ With the flux of these defects being biased by strain and the vacancy hydrogenation processes being exothermic, one expects that vacancy-hydrogen defects will plate out in the region of high stress. The dipole tensile field should ultimately lead to the growth of platelets on planes that are perpendicular to the out-of-plane strain direction. Platelets oriented in the other two directions are disfavored by the attendant superposed compressive strains.

The nucleation of {111} platelets during hydrogenation of Si was discussed by Johnson *et al.*¹⁸ where the nucleation

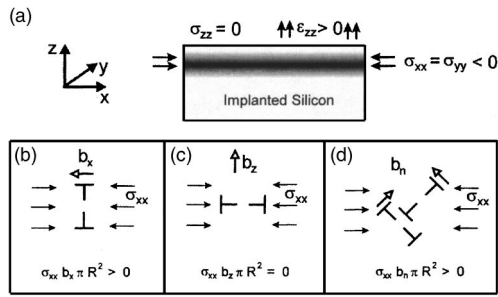


FIG. 3. Schematic representation of the biaxial in-plane stress state in the hydrogen ion implanted Si substrates (a) and the influence of this applied stress, through the term $-\sigma_{xx} b_n \pi R^2$ (Eq. (3)), on the nucleation and growth of hydrogen platelets with different orientations (b) – (d). For σ_{xx} or σ_{yy} negative and the platelet surface normal to the x or y direction ($n = x, y$), $\sigma_{xx} b_n$ will be positive and there will be an additional barrier to any platelet not nucleating in the plane of stress (b). When the stress σ_{xx} and Burgers vector b_n are orthogonal, there will be no effect on platelets nucleating with their surface normal to the z direction (c). The σ_{xx} or σ_{yy} stress acting on $\{111\}$ platelets not parallel to the surface in (111) hydrogen ion implanted Si also adds an additional barrier to platelet nucleation. Once nucleated, Eq. (3) will favor or disfavor platelet growth in the same way that it affects platelet nucleation.

of platelets in Si supersaturated with hydrogen was qualitatively described using a Volmer-type theory. The model proposed by Johnson considered a circular nucleus of radius R forming on a particular plane. The total free energy change upon nucleation of the H platelet of radius R and thickness t was expressed as

$$\Delta G(R) = -\pi R^2 t \Delta G_v + 2\pi R \gamma t + 2\pi R c \ln(R), \quad (2)$$

where ΔG_v is the energy difference per unit volume between the supersaturated state and the platelet state, $2\pi R \gamma t$ is the perimeter energy of the platelet nuclei (γ =surface energy), and $2\pi R c \ln(R)$ is the strain energy resulting from formation of nuclei in the Si lattice (with c a constant), which was modeled as the self-energy of a dislocation loop of radius R . In general, a term $2\pi R^2 \gamma_2$ should be added to Eq. (2) to account for the surface energy γ_2 of the platelet surface. Equation (2), so modified, is sufficient to describe the nucleation process in the absence of applied stresses. However, hydrogen ion implanted Si is in a state of biaxial compressive stress ($\sigma_{xx} = \sigma_{yy} < 0, \sigma_{zz} = 0$),^{2,9} Figure 3(a), which would add an additional term to Eq. (2) of the form¹⁹

$$-\int_0^R \sigma_{nn} b_n 2\pi r dr = -\sigma_{nn} b_n \pi R^2, \quad (3)$$

where b_n is the Burgers vector of the platelet loop, σ_{nn} is the externally applied stress (i.e., in-plane residual stress in our case) acting on the platelet, and $\sigma_{nn} b_n$ is a tensor product. Equation (3) will be zero when the stress and Burgers vector are orthogonal, indicating that there will be no effect from Eq. (3) on platelets nucleating with their surface normal to the z direction, Fig. 3(c). However, when the platelet surface is normal to the x or y direction, $n = x, y$, and for σ_{xx} or σ_{yy} negative, Eq. (3) will be positive, Fig. 3(b). Therefore, there is an energetic barrier to any platelet not nucleating in the plane of stress. This explains why the predominant (111)

platelets observed in (111) hydrogen ion implanted Si (Fig. 2) are parallel to the surface, while all variants of $\{111\}$ platelets are observed in hydrogenated Si where $\sigma_{nn} = 0$ for all orientations, Fig. 3(d). This same reasoning also explains platelet morphology observed in hydrogen ion implanted (100) Si. Once nucleated, the $\sigma_{nn} b_n$ term in Eq. (3) still favors or disfavors platelet growth. Thus both nucleation and growth are affected by the stress produced by the ion implantation.

We have shown that the out-of-plane tensile strain present in hydrogen ion implanted Si provides a driving force for vacancy migration to the region of highest tensile strain. The platelet distribution coincides with the strain distribution, indicating hydrogenated vacancies provide the nuclei for platelet formation. Further, we have shown that the platelet nucleation is strongly dependent on applied stresses and that the in-plane compressive stress that results from ion implantation damage favors both the nucleation and growth of platelets that are in the plane of stress and parallel to the sample surface.

Discussions with Greg Swadener, S. S. Lau, and J. W. Mayer are gratefully acknowledged. This work was supported by the U.S. Department of Energy, Office of Basic Energy Sciences.

- ¹N. H. Nickel, G. B. Anderson, N. M. Johnson, and J. Walker, Phys. Rev. B **62**, 8012 (2000).
- ²T. Höchbauer, A. Misra, M. Nastasi, and J. W. Mayer, J. Appl. Phys. **89**, 5980 (2001).
- ³M. Wormington, C. Panaccione, K. M. Matney, and K. Bowen, Philos. Trans. R. Soc. London, Ser. A **357**, 2827 (1999), and references therein.
- ⁴M. Nastasi, T. Höchbauer, R. D. Verda, A. Misra, J. K. Lee, J. W. Mayer, and S. S. Lau, Nucl. Instrum. Methods Phys. Res. B, **219/220**, 604 (2004).
- ⁵R. D. Verda, J. R. Tesmer, M. Nastasi, and R. W. Bower, Nucl. Instrum. Methods Phys. Res. B **187**, 383 (2002).
- ⁶R. D. Verda, J. R. Tesmer, M. Nastasi, and R. W. Bower, Nucl. Instrum. Methods Phys. Res. B **190**, 419 (2002).
- ⁷V. S. Sperious, B. M. Paine, M-A. Nicolet, and H. L. Glass, Appl. Phys. Lett. **40**, 604 (1982).
- ⁸V. D. Tkachev, G. Holzer, and A. R. Chelyadinskii, Phys. Status Solidi A **85**, k43 (1984).
- ⁹Y. Zheng, S. S. Lau, T. Höchbauer, A. Misra, R. Verda, X. M. He, M. Nastasi, and J. W. Mayer, J. Appl. Phys. **89**, 2972 (2001).
- ¹⁰T. Höchbauer, M. Nastasi, and J. W. Mayer, Appl. Phys. Lett. **75**, 3938 (1999).
- ¹¹T. Höchbauer, A. Misra, R. Verda, M. Nastasi, J. W. Mayer, Y. Zheng, and S. S. Lau, Philos. Mag. B **80**, 1921 (2000).
- ¹²T. Höchbauer, A. Misra, R. Verda, Y. Zheng, S. S. Lau, J. W. Mayer, and M. Nastasi, Nucl. Instrum. Methods Phys. Res. B **175–177**, 169 (2001).
- ¹³F. A. Reboredo, M. Ferconi, and S. T. Pantelides, Phys. Rev. Lett. **82**, 4870 (1999).
- ¹⁴J. P. Hirth and J. Lothe, *Theory of Dislocations* (Wiley, New York, 1982), Chap. 2.
- ¹⁵P. G. Shewmon, *Diffusion in Solids* (McGraw-Hill, New York, 1963), Chap. 1.
- ¹⁶G. D. Watkins, in *Handbook of Semiconductor Technology*, edited by K. A. Jackson and W. Schroter (Wiley-VCH, Weinheim, 2000), p.123.
- ¹⁷M. A. Robertson and S. K. Estreicher, Phys. Rev. B **49**, 17040 (1994).
- ¹⁸N. M. Johnson, C. Herring, C. Doland, J. Walker, G. Anderson, and F. Ponce, Mater. Sci. Forum **83**, 33 (1992).
- ¹⁹The elastic field of the platelet is well described as that of a prismatic dislocation loop growing in the presence of a Peach-Koehler force σb , where σ is the applied stress and b is the Burger's vector of the dislocation.